Available online at www.sciencedirect.com
SCIENCE DIRECT®
Combustion and Flame 136 (2004) 208–216
Combustion and Flame
www.elsevier.com/locate/jnlabr/cnf

An investigation of the performance of turbulent mixing models

Zhuyin Ren * and Stephen B. Pope

Sibley School of Mechanical and Aerospace Engineering, Cornell University, Ithaca, NY 14853, USA

Received 13 April 2003; received in revised form 15 September 2003; accepted 15 September 2003

Abstract

Modeling of partially stirred reactors (PaSR) by stochastic Monto Carlo simulations is carried out to investigate the relative performance of three existing turbulent mixing models: the interaction by exchange with the mean model, the modified Curl mixing model, and the Euclidean minimum spanning tree model. A detailed mechanism for hydrogen oxidation, which involves 9 species and 19 reactions, is incorporated into the simulations using the *in situ* adaptive tabulation algorithm. Numerical simulations are performed for a wide range of residence and mixing times revealing the significant differences in the PDFs of mixture fraction, in the scatter plots, and in the extinction behaviors between the three different mixing models. The conditional mean scalar dissipation implied by each model is deduced analytically or numerically in the PaSR, but it is shown not to have the same significance as in the conditional moment closure and flamelet models.

Keywords: Turbulent nonpremixed flames; Numerical simulations

1. Introduction

In the modeling of turbulent reactive flows based on PDF methods, the change in fluid composition due to reaction is treated exactly, while molecular mixing has to be modeled. Modeling mixing in particle implementations of PDF methods involves prescribing the evolution of stochastic/conditional particles in composition space such that they mimic the change in the composition of a fluid particle due to mixing in a turbulent reactive flow.

Mixing models are essential for PDF methods and previous calculations show sensitivity of piloted flame results to the choice of mixing model. Calculations of the Barlow and Frank [1] piloted-jet methane/air flame F performed by different groups, especially by Tang et al. [2], by Xu and Pope [3], and by Lindstedt et al. [4], demonstrate the sensitivity of extinction results to the choice of the mixing model and constants.

In order to investigate the relative performance of different mixing models for nonpremixed turbulent reactive flows, this work examines the performance of three different existing mixing models: the interaction by exchange with the mean (IEM or LMSE) model [5,6], the modified Curl mixing (MC) model [7], and the Euclidean minimum spanning tree (EMST) model [8]. The idealized partially stirred reactor (PaSR) is studied for simplicity. It is similar to a single grid cell embedded in a large PDF computation of nonpremixed turbulent combustion. Similarly we consider a single diluted H_2–air case as a function of the two time scales: the residence time τ_{res} and the mixing time τ_{mix}. We first study the PDFs of the mixture fraction ξ, the scatter plots, and the extinction behaviors to reveal the differences between the three mixing models. In Appendices A and B, we derive analytic expressions for the Favre mean and variance

* Corresponding author.
E-mail address: zr26@cornell.edu (Z. Ren).

0010-2180/$ – see front matter
doi:10.1016/j.combustflame.2003.09.014

of mixture fraction ξ and the conditional mean scalar dissipation implied by the IEM model for the PaSR in the statistically stationary state. We show that the conditional mean scalar dissipation implied by the IEM model does not have the same significance as in the conditional moment closure (CMC) and flamelet models.

2. Test case: partially stirred reactor

It is supposed that the adiabatic PaSR is continuously fed by two inlets, which inject cold nonpremixed fuel and oxidant into the reactor at the mass flow rates $\dot{m}_{\mathrm{fu}}$ and $\dot{m}_{\mathrm{ox}}$, respectively. In our simulations, the two inflow streams are the fuel stream (H_2 and N_2, 1 : 1 by volume, $T = 300$ K) and the oxidant stream (N_2 and O_2, 79 : 21 by volume, $T = 300$ K). The pressure is atmospheric throughout. Inside the reactor, reaction occurs and the mean thermochemical properties are assumed to be statistically spatially homogeneous, but the fluid is imperfectly mixed at the molecular level. Simultaneously, the resulting mixture is withdrawn from the reactor at a rate equal to the total mass inflow rates, i.e., $\dot{m} = \dot{m}_{\mathrm{ox}} + \dot{m}_{\mathrm{fu}}$. The mass of fluid inside the reactor, m, is constant; so the mean residence time τ_{res} can be defined as $\tau_{\mathrm{res}} = m/\dot{m}$. The inflow mass fraction of the oxidant stream, P, is defined as $P = \dot{m}_{\mathrm{ox}}/[\dot{m}_{\mathrm{ox}} + \dot{m}_{\mathrm{fu}}]$. In the PaSR, when statistically stationary, the equivalence ratio Φ is related to P through $\Phi = (1-P)/(1-P_{\mathrm{st}})$, where P_{st} is the value of P when the inflow mixture yields stoichiometry. In our simulations, P_{st} is equal to 0.696. The composition $\boldsymbol{\phi}$ consists of species mass fractions and enthalpy, and it determines the thermochemical state of the mixture. We use $\boldsymbol{\psi}$ as the sample-space variable corresponding to $\boldsymbol{\phi}$ and use $\boldsymbol{\phi}^0$ and $\boldsymbol{\phi}^1$ to denote the compositions of the inflow oxidant and fuel streams, respectively.

With the assumption of equal diffusivities Γ, the transport equation for the density-weighted joint PDF, $\tilde{f}(\boldsymbol{\psi}; t) = \rho(\boldsymbol{\psi})\langle\delta(\boldsymbol{\psi} - \boldsymbol{\phi})\rangle/\langle\rho(\boldsymbol{\phi})\rangle$, is [9]

$$\begin{aligned}\frac{\partial \tilde{f}}{\partial t} &= -\frac{\tilde{f}}{\tau_{\mathrm{res}}} \\ &\quad + \frac{1}{\tau_{\mathrm{res}}}\big[P\delta\big(\boldsymbol{\phi}^0 - \boldsymbol{\psi}\big) + (1-P)\delta\big(\boldsymbol{\phi}^1 - \boldsymbol{\psi}\big)\big] \\ &\quad - \frac{\partial}{\partial \psi_\alpha}\big[\tilde{f} S_\alpha(\boldsymbol{\psi})\big] \\ &\quad - \frac{\partial^2}{\partial \psi_\alpha \psi_\beta}\left[\tilde{f}\left\langle \Gamma \frac{\partial \phi_\alpha}{\partial x_i}\frac{\partial \phi_\beta}{\partial x_i}\,\middle|\,\boldsymbol{\psi}\right\rangle\right], \end{aligned} \tag{1}$$

where ρ is density, S_α is the source term due to reaction, and the summation convention applies. In Eq. (1), the first three terms on the right-hand side represent the effects of outflow, inflow, and chemical reaction, respectively, on the joint PDF: these processes require no modeling. The last term represents the effect of microscale mixing on the joint PDF: each of the three mixing models considered is intended to model this process.

In the stochastic simulation of the PaSR, a time marching scheme is used to solve Eq. (1) (with the final term replaced by a model). At any time t, the PaSR consists of $N = 1000$ particles, the ith particle having composition $\boldsymbol{\phi}^{(i)}(t)$, weight $w^{(i)}$, and age $s^{(i)}$ (which is the elapsed time since the particle entered the reactor). In our simulations, all particles have equal weights. With Δt being the specified time step, at the discrete times $k\Delta t$ (k integer) events occur corresponding to *inflow* and *outflow*, which can cause $\boldsymbol{\phi}^{(i)}(t)$ to change discontinuously. Between these discrete times, the composition evolves by a *mixing* fractional step and a *reaction* fractional step. These processes are now described in more detail.

(1) Inflow/outflow: Choose $N_{\mathrm{replaced}} (= N \times \Delta t/\tau_{\mathrm{res}})$ particles randomly with replacement from the ensemble of N particles, replace them with an equal number of particles from the inflow streams, and reset their ages to zero. This procedure leads to a theoretical age distribution given by an exponential form $f_{\mathrm{age}}(s) = \frac{1}{\tau_{\mathrm{res}}}\exp(-s/\tau_{\mathrm{res}})$ [10] with an average age of τ_{res} for $\Delta t \to 0$.

(2) Mixing fractional step: Mixing models are used to model molecular mixing. In this fractional step, the mixing time τ_{mix} is the characteristic time scale and is defined to yield a particular decay of variance. For IEM [5,6], the ordinary differential equation,

$$\frac{d\boldsymbol{\phi}^{(i)}}{dt} = -\frac{(\boldsymbol{\phi}^{(i)} - \tilde{\boldsymbol{\phi}})}{2\tau_{\mathrm{mix}}}, \tag{2}$$

is solved for each particle over a period of Δt, where $\tilde{\boldsymbol{\phi}}$ is the Favre mean composition of the ensemble of particles. In MC [7] with equal-weight particles, $N \times \frac{\Delta t}{\tau_{\mathrm{mix}}}$ pairs of particles are randomly selected with replacement from the ensemble and mixing occurs within each pair according to

$$\begin{aligned}\boldsymbol{\phi}^{(p,new)} &= \boldsymbol{\phi}^{(p)} + \frac{1}{2}a\big(\boldsymbol{\phi}^{(q)} - \boldsymbol{\phi}^{(p)}\big), \\ \boldsymbol{\phi}^{(q,new)} &= \boldsymbol{\phi}^{(q)} + \frac{1}{2}a\big(\boldsymbol{\phi}^{(p)} - \boldsymbol{\phi}^{(q)}\big), \end{aligned} \tag{3}$$

where p and q denote the pair of particles and a is a random variable uniformly distributed in $(0, 1)$. EMST [8,11] is a complicated particle-interaction model, loosely based on the form of the mapping closure particle equations, which uses the Euclidean minimum spanning trees in composition space. In this model, the change in particle composition is determined by particle interactions along the edges of Euclidean minimum spanning tree constructed on the

Table 1
Reaction mechanism of the H_2/air system [12]

		A	β	E_a
R1	$O_2 + H \Leftrightarrow OH + O$	2.00×10^{14}	0.0	70.3
R2	$H_2 + O \Leftrightarrow OH + H$	5.06×10^{4}	2.7	26.3
R3	$H_2 + OH \Leftrightarrow H_2O + H$	1.00×10^{8}	1.6	13.8
R4	$OH + OH \Leftrightarrow H_2O + O$	1.50×10^{9}	1.1	0.4
R5	$H + H + M \Leftrightarrow H_2 + M$	1.80×10^{18}	−1.0	0.0
R6	$H + OH + M \Leftrightarrow H_2O + M$	2.20×10^{22}	−2.0	0.0
R7	$O + O + M \Leftrightarrow O_2 + M$	2.90×10^{17}	−1.0	0.0
R8	$H + O_2 + M \Leftrightarrow HO_2 + M$	2.30×10^{18}	−0.8	0.0
R9	$HO_2 + H \Leftrightarrow OH + OH$	1.50×10^{14}	0.0	4.2
R10	$HO_2 + H \Leftrightarrow H_2 + O_2$	2.50×10^{13}	0.0	2.9
R11	$HO_2 + H \Leftrightarrow H_2O + O$	3.00×10^{13}	0.0	7.2
R12	$HO_2 + O \Leftrightarrow OH + O_2$	1.80×10^{13}	0.0	−1.7
R13	$HO_2 + OH \Leftrightarrow H_2O + O_2$	6.00×10^{13}	0.0	0.0
R14	$HO_2 + HO_2 \Rightarrow H_2O_2 + O_2$	2.50×10^{11}	0.0	−5.2
R15	$OH + OH + M \Leftrightarrow H_2O_2 + M$	3.25×10^{22}	−2.0	0.0
R16	$H_2O_2 + H \Leftrightarrow H_2 + HO_2$	1.70×10^{12}	0.0	15.7
R17	$H_2O_2 + H \Leftrightarrow H_2O + OH$	1.00×10^{13}	0.0	15.0
R18	$H_2O_2 + O \Leftrightarrow OH + HO_2$	2.80×10^{13}	0.0	26.8
R19	$H_2O_2 + OH \Leftrightarrow H_2O + HO_2$	5.40×10^{12}	0.0	4.2

A units, mol cm s K; E_a units, kJ/mol; $k^+ = AT^\beta \exp(-E_a/\mathcal{R}T)$, mol cm s K.

ensemble of particles in composition space. Consequently, the mixing is modeled locally in composition space.

(3) Reaction fractional step: Each particle evolves by the reaction equation

$$\frac{d\boldsymbol{\phi}^{(i)}}{dt} = S\big(\boldsymbol{\phi}^{(i)}\big), \tag{4}$$

over a period of Δt. The detailed mechanism [12] (see Table 1) for hydrogen oxidation, which involves 9 species and 19 reactions, is incorporated into the simulations using the *in situ* adaptive tabulation (ISAT) algorithm [13]. The ISAT error tolerance, ε_{tol}, is set to 1.0×10^{-5}, which guarantees less than 1% tabulation error for all species in our calculation.

In our simulations, the initial condition is that all particles are in chemical equilibrium: 60% of the particles have the stoichiometric mixture fraction ξ_{st} ($= 0.304$), and the remaining 40% of the particles are uniformly distributed based on mixture fraction. The time step Δt is chosen to be $\frac{1}{10}\min(\tau_{\text{res}}, \tau_{\text{mix}})$ in order to ensure numerical accuracy.

For convenience, we introduce conditional Favre averaging: $\langle\cdot|\eta\rangle_\rho \equiv \langle\cdot\rho|\eta\rangle/\langle\rho|\eta\rangle$, where ρ is density and η is the sample-space variable corresponding to mixture fraction. In the PaSR, when statistically stationary, for the IEM model there are no conditional fluctuations, and hence there is no difference between the unweighted conditional averages and the conditional Favre averages, i.e., $\langle\cdot|\eta\rangle_\rho = \langle\cdot|\eta\rangle$, because all quantities (ρ, $\boldsymbol{\phi}$, etc.) are deterministic functions of η.

In the following section, we present the results when the PaSR has reached statistical stationarity. The quantities conditional on the mixture being stoichiometric are estimated according to $\langle\cdot|\xi_{\text{st}}\rangle_\rho = \int_{\xi_{\text{st}}-0.05}^{\xi_{\text{st}}+0.05} \tilde{p}(\eta)\langle\cdot|\eta\rangle_\rho \, d\eta / \int_{\xi_{\text{st}}-0.05}^{\xi_{\text{st}}+0.05} \tilde{p}(\eta)\, d\eta$, i.e., the range of ξ used to estimate the quantities conditional on the mixture being stoichiometric is from 0.254 to 0.354. Here $\tilde{p}(\eta)$ is the PDF of mixture fraction, $\tilde{p}(\eta) = \langle\rho|\eta\rangle\langle\delta(\eta-\xi)\rangle/\langle\rho\rangle$.

3. Results and discussion

3.1. Effect of $\tau_{\text{mix}}/\tau_{\text{res}}$ on the PDF of mixture fraction

As shown in Appendix A, when statistically stationary, the Favre mean and variance of mixture fraction in the PaSR are

$$\tilde{\xi} = 1 - P \tag{5}$$

and

$$\widetilde{\xi''^2} = P(1-P)/(1+\tau_{\text{res}}/\tau_{\text{mix}}). \tag{6}$$

These results hold for all of the mixing models, except that (as discussed in Appendix A) Eq. (6) is satisfied only to an approximation in EMST.

As the ratio $\tau_{\text{mix}}/\tau_{\text{res}}$ increases, $\widetilde{\xi''^2}$ increases and the PDF of mixture fraction evolves from one delta function (at $\eta = \tilde{\xi}$, for $\tau_{\text{mix}}/\tau_{\text{res}} \to 0$, which is the

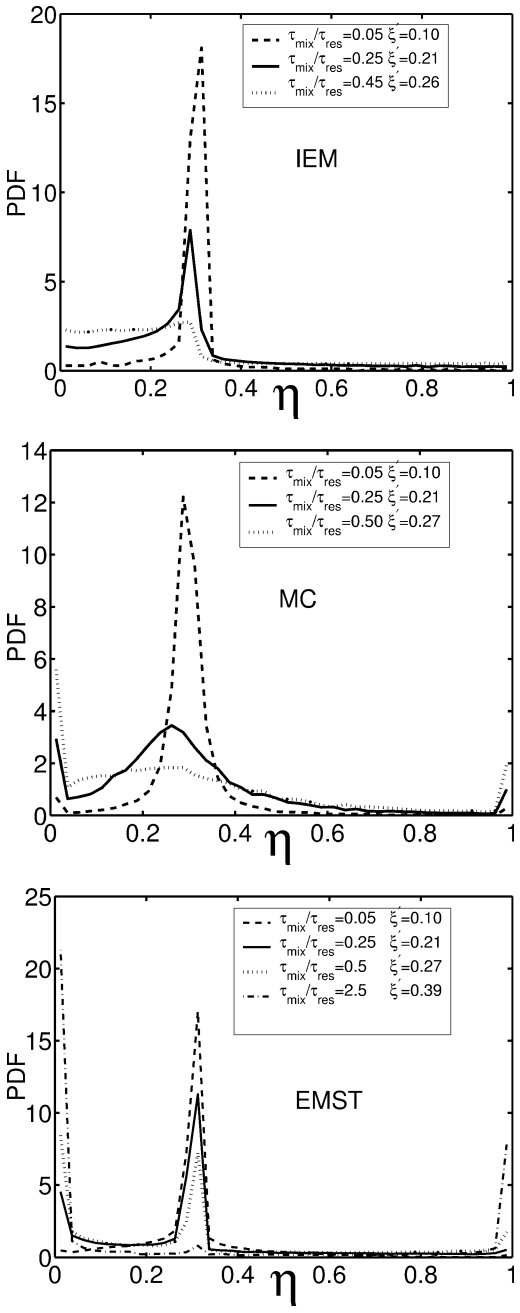

Fig. 1. PDFs of mixture fraction given by the three models for different values of $\tau_{\mathrm{mix}}/\tau_{\mathrm{res}}$ and $\tau_{\mathrm{res}} = 2 \times 10^{-3}$ (s). The values of the Favre-averaged rms ξ' are shown in the keys.

PSR limit) toward two delta functions (at $\eta = 0$ and $\eta = 1$, for $\tau_{\mathrm{mix}}/\tau_{\mathrm{res}} \to \infty$, which is the unmixed limit).

Figure 1 shows the PDFs given by the three mixing models for several intermediate values of $\tau_{\mathrm{mix}}/\tau_{\mathrm{res}}$ with $\tau_{\mathrm{res}} = 2 \times 10^{-3}$ (s) and $\Phi = 1.0$. The figure shows that for the same values of $\tilde{\xi}$ and $\widetilde{\xi''^2}$ (resulting from the same values of P and $\tau_{\mathrm{mix}}/\tau_{\mathrm{res}}$), the PDFs of the mixture fraction for the three different mixing models are quite different. The EMST model results in a relatively higher probability around stoichiometry when $\widetilde{\xi''^2}$ increases. For other equivalence ratios ($\Phi = 0.7$ and $\Phi = 1.3$, not shown), we obtain conclusions similar to that for $\Phi = 1.0$.

3.2. Scatter plots

Figure 2 shows the scatter plots of temperature against mixture fraction η, which are obtained with $\tau_{\mathrm{res}} = 2 \times 10^{-3}$ (s), $\tau_{\mathrm{mix}}/\tau_{\mathrm{res}} = 0.35$, and $\Phi = 1.0$. The lines in the scatter plots correspond to chemical equilibrium. Note from Fig. 2a that the reaction zone in mixture fraction space is from about 0.24 to about 0.5. The scatter below the equilibrium line in the reaction zone corresponds to incompletely burned particles or extinguished particles. In this case, τ_{res} is at least an order of magnitude greater than the extinction value (see Fig. 3b) and little local extinction is to be expected.

Figure 2 shows the qualitatively different behavior of the three mixing models. For the IEM model, Fig. 2a is consistent with the following picture: particles corresponding to composition values outside the reaction zone relax to the mean composition and are drawn away from their initial condition on the equilibrium line; particles in the reaction zone react back close to their equilibrium values due to fast reactions. It is clear that particles do not all lie close to the equilibrium line and the model fails to reproduce the expected physical behavior in this case. Figure 2b shows that the MC model mixes cold fuel with cold oxidant to produce cold, nonreactive mixtures which are within the reaction zone in mixture-fraction space. Clearly, this is physically incorrect in this case. Figure 2c shows that all compositions given by the EMST model for this case are close to equilibrium. So Fig. 2 shows that the EMST mixing model produces the expected physical behavior, whereas the IEM model and MC model do not. The corresponding mixture-fraction PDFs are also shown in Fig. 2 and they are quite different.

3.3. Extinction results

In the PaSR, the inflow mixtures are nonpremixed cold fuel and cold oxidant. Global extinction occurs for a fixed value of $\tau_{\mathrm{mix}}/\tau_{\mathrm{res}}$ when τ_{res} is reduced to a point at which chemical reaction cannot be sustained. Also global extinction occurs as τ_{mix} increases (for a fixed value of τ_{res}) due to insufficient mixing. The mean temperature conditional on the mixture being stoichiometric, $\langle T|\xi_{\mathrm{st}}\rangle_{\rho}$, is a sensitive measure of

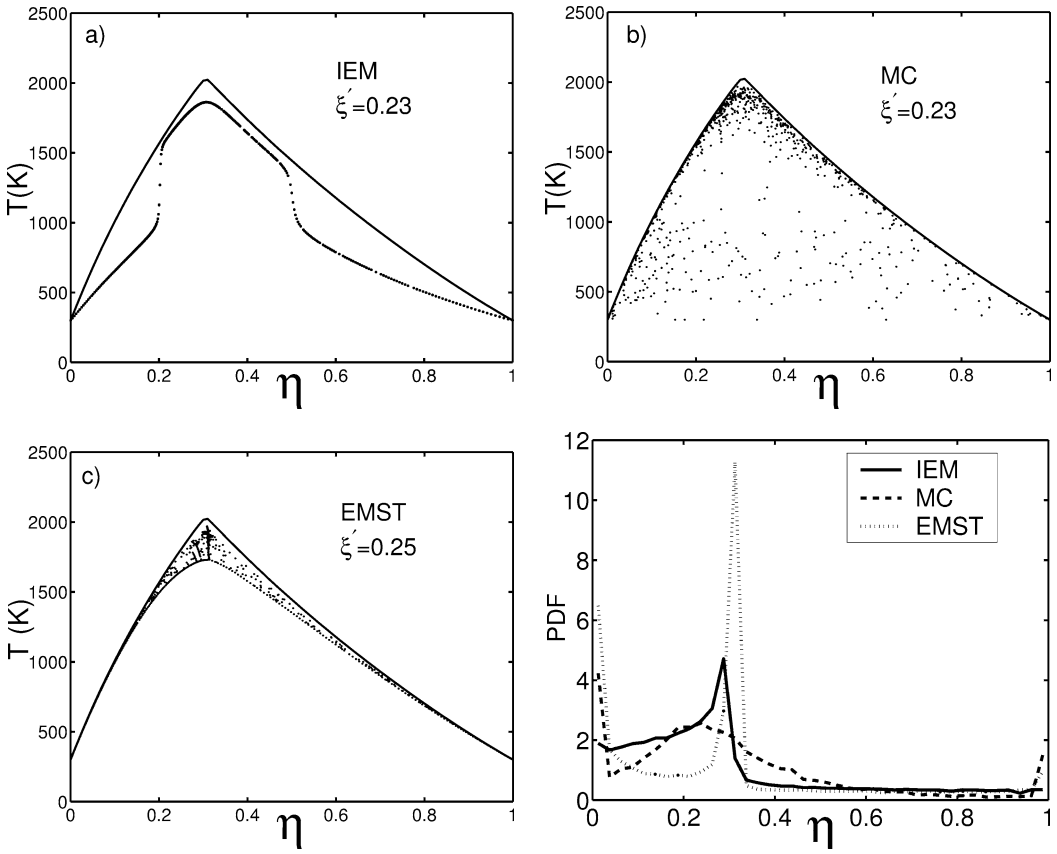

Fig. 2. Scatter plots of temperature T against mixture fraction η and the corresponding PDFs of mixture fraction obtained with $\tau_{\text{res}} = 2 \times 10^{-3}$ (s) and $\tau_{\text{mix}}/\tau_{\text{res}} = 0.35$. The lines in the scatter plots correspond to chemical equilibrium.

the approach to extinction. Here we use $\langle T|\xi_{\text{st}}\rangle_\rho$ to study the above two extinction behaviors for the three mixing models (for $\Phi = 1.0$).

Figures 3a and 3b show $\langle T|\xi_{\text{st}}\rangle_\rho$ for different values of τ_{res}, for fixed $\tau_{\text{mix}}/\tau_{\text{res}}$. Figure 3c shows $\langle T|\xi_{\text{st}}\rangle_\rho$ for different values of τ_{mix}, for fixed τ_{res}. The asterisk symbol in the figure is the corresponding extinction point. Figure 3 shows that the three mixing models are in good agreement with each other for small Favre-averaged rms mixture fraction ξ'' (small $\tau_{\text{mix}}/\tau_{\text{res}}$), but considerable differences arise for large ξ'' (large $\tau_{\text{mix}}/\tau_{\text{res}}$). The EMST model is more resistant to global extinction than the IEM and MC models. For other equivalence ratios ($\Phi = 0.7$ and $\Phi = 1.3$, not shown) we obtain conclusions similar to that for $\Phi = 1.0$.

3.4. Implied conditional mean scalar dissipation

The scalar dissipation of mixture fraction χ (defined as $\chi = 2\Gamma \nabla\xi \cdot \nabla\xi$) and its statistics (its PDF, variance, conditional mean, etc.) are important quantities in most modeling approaches to nonpremixed turbulent combustion such as the CMC [14] and flamelet models [15]. In the following two subsections, the conditional mean scalar dissipation of mixture fraction $\langle \chi|\eta\rangle_\rho$ implied by the three mixing models in the PaSR is derived, compared, and shown not to have the same significance as in the CMC and flamelet models.

In the PaSR, the implied Favre mean scalar dissipation is

$$\tilde{\chi} = \widetilde{\xi''^2}/\tau_{\text{mix}}, \tag{7}$$

and $\tilde{\chi}$ and $\langle \chi|\eta\rangle_\rho$ are related through

$$\tilde{\chi} = \int_0^1 \langle \chi|\eta\rangle_\rho \, \tilde{p}(\eta)\, d\eta, \tag{8}$$

where $\tilde{p}(\eta)$ is the density-weighted PDF of ξ and $\langle \chi|\eta\rangle_\rho/\tilde{\chi}$ depends only on $\tau_{\text{mix}}/\tau_{\text{res}}$, P (or Φ), η, and the model.

According to Eq. (6), $\widetilde{\xi''^2}$ is determined by $\tau_{\text{mix}}/\tau_{\text{res}}$ and P. So, given the same values of $\tau_{\text{mix}}/\tau_{\text{res}}$, P, and τ_{mix}, $\tilde{\chi}$ is the same for the three mixing models.

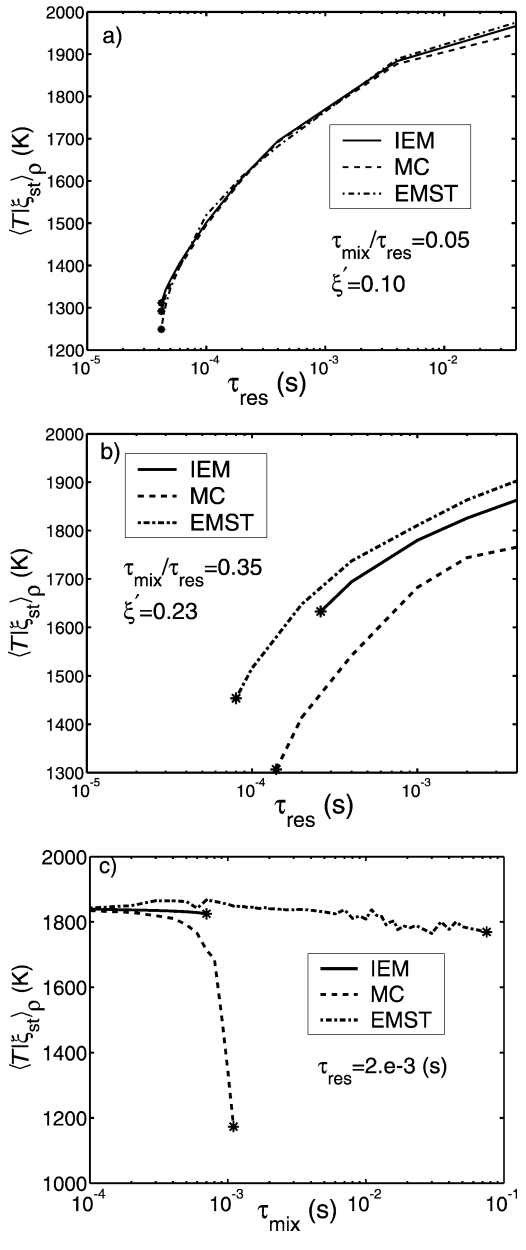

Fig. 3. (a and b) Mean temperature conditional on stoichiometric mixture fraction against residence time for fixed values of $\tau_{\mathrm{mix}}/\tau_{\mathrm{res}}$ (c) $\langle T|\xi_{\mathrm{st}}\rangle_\rho$ against τ_{mix} for $\tau_{\mathrm{res}} = 2 \times 10^{-3}$ (s). The extinction point is indicated by an asterisk.

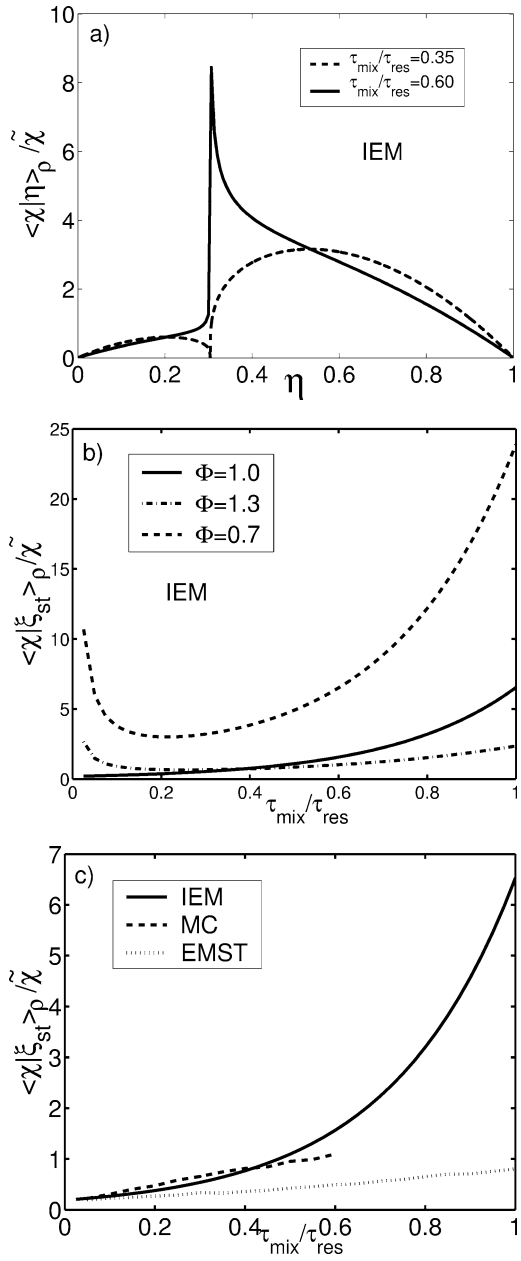

Fig. 4. (a) The distribution of the implied value of $\langle\chi|\eta\rangle_\rho/\tilde{\chi}$ for the IEM model (obtained analytically) with $\Phi = 1.0$. (b) Implied value of $\langle\chi|\xi_{\mathrm{st}}\rangle_\rho/\tilde{\chi}$ for different values of Φ for the IEM model. (c) Implied values of $\langle\chi|\xi_{\mathrm{st}}\rangle_\rho/\tilde{\chi}$ for different mixing models (obtained numerically) for $\Phi = 1.0$.

However, the implied conditional mean scalar dissipation distribution is quite different.

For the IEM model in the statistically stationary state, as shown in Appendix B, we obtain an analytical expression for the PDF of mixture fraction (Eq. (17)) and then derive an analytical expression for the implied value of $\langle\chi|\eta\rangle_\rho$ (Eq. (22)) from the PDF balance equation. For the MC and EMST models in the statistically stationary state, we can obtain numerical values of the PDFs of mixture fraction through simulations. Then, by numerically integrating the PDF balance equation twice, we can obtain the implied conditional mean scalar dissipation of mixture fraction.

Figures 4a and 4b show the distribution of $\langle\chi|\eta\rangle_\rho/\tilde{\chi}$ and $\langle\chi|\xi_{\rm st}\rangle_\rho/\tilde{\chi}$ for the IEM model under different conditions. Figure 4c shows $\langle\chi|\xi_{\rm st}\rangle_\rho/\tilde{\chi}$ for the three mixing models as functions of $\tau_{\rm mix}/\tau_{\rm res}$ for $\Phi = 1$. Figure 4 shows that, even for the same mixing model, the distribution of conditional mean scalar dissipation changes significantly when $\tau_{\rm mix}/\tau_{\rm res}$ or Φ is changed. Figure 4 also shows that when $\tau_{\rm mix}/\tau_{\rm res}$ is increased, large differences arise among the three mixing models. These results are consistent with the extinction results.

3.5. Relevance of conditional mean scalar dissipation implied by the IEM model

In the PaSR when statistically stationary, for the IEM model, all quantities are deterministic functions of η, so there are no conditional fluctuations and $\langle\cdot|\eta\rangle_\rho$ is equal to $\langle\cdot|\eta\rangle$. Furthermore, taking the mass fraction $Y_{\rm H_2O}$ as the progress variable and following the procedure in [14], the CMC model equation for the conditional mean of the progress variable is

$$S(\eta, Q) = -\frac{1}{2}\langle\chi|\eta\rangle_\rho \frac{\partial^2 Q}{\partial\eta^2}, \tag{9}$$

where $Q(\eta)$ denotes $\langle Y_{\rm H_2O}|\eta\rangle_\rho$ and $S(\eta, Q)$ is the reaction rate.

If the conditional mean scalar dissipation implied by the IEM model has the same significance as in CMC and flamelet theories, the CMC model equation should hold. But this is not the case. Figure 5 clearly shows that the equation does not hold (very obviously in the rectangular region: the left-hand side of the equation is positive, whereas the right-hand side is negative). So the implied conditional mean scalar dissipation by the IEM model does not have the same significance as in CMC and flamelet theories. The reason is as follows.

In both CMC and simple flamelet theory, the reaction progress variable is related to mixture fraction by a relation of the form $Y_{\rm H_2O}(\mathbf{x}, t) = Q(\xi[\mathbf{x}, t])$. Consequently the diffusive fluxes are linked by

$$\Gamma\nabla Y_{\rm H_2O} = \Gamma\nabla\xi\, Q'(\xi), \tag{10}$$

where Q' denotes the derivative of Q, and the CMC equation (Eq. (9)) stems from this linkage. But the IEM model does not contain this linkage, and so its results do not conform to Eq. (9).

In the combustion regimes in which CMC and flamelet models are well founded, these models accurately represent the coupled process of reaction and molecular diffusion. In these circumstances, the IEM model does not contain the correct coupling (e.g., Eq. (10)), and consequently can be expected to be less accurate.

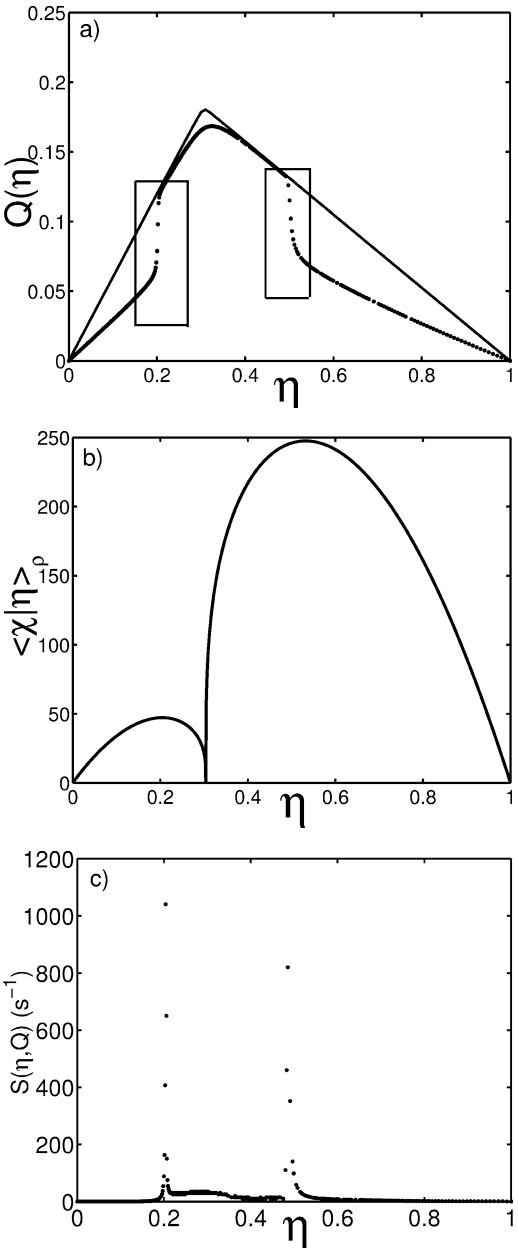

Fig. 5. (a) The expectation of $Y_{\rm H_2O}$ conditional on $\xi = \eta$ against mixture fraction. (b) The distribution of the implied value of $\langle\chi|\eta\rangle_\rho$. (c) Reaction rate against mixture fraction. All results were obtained for the IEM model with $\tau_{\rm res} = 2\times10^{-3}$ (s), $\tau_{\rm mix}/\tau_{\rm res} = 0.35$, and $\Phi = 1.0$.

4. Conclusions

The PaSR test reveals several important differences in the performance of the three mixing models (IEM, MC, and EMST). For given values of $\tau_{\rm mix}/\tau_{\rm res}$ and P, the Favre mean and variance of mixture fraction are almost the same for all models, but the PDFs

are significantly different: the EMST model results in a relatively higher probability around stoichiometry when ξ' is increased. For the same conditions, scatter plots reveal the qualitatively different behavior of the three mixing models. Except at small values of ξ', the models exhibit substantially different extinction behaviors: the EMST model is more resistant to global extinction than the IEM and MC models. The implied conditional mean scalar dissipation can be deduced for each model analytically or numerically, but it does not have the same significance as in the CMC and flamelet models.

Acknowledgment

This work is supported in part by Department of Energy, Grant DE-FG02-90ER14128.

Appendix A. Determination of the Favre mean and variance of mixture fraction in the PaSR

In the PaSR, when statistically stationary, the transport equation for the PDF of mixture fraction, $\tilde{p}(\eta)$, is

$$\begin{aligned}\frac{\partial \tilde{p}(\eta)}{\partial t} &= 0 \\ &= -\frac{\tilde{p}(\eta)}{\tau_{\text{res}}} + \frac{1}{\tau_{\text{res}}}\big[P\delta(\eta) + (1-P)\delta(1-\eta)\big] \\ &\quad - \frac{\partial^2}{\partial \eta^2}\left(\frac{1}{2}\tilde{p}(\eta)\langle\chi|\eta\rangle_\rho\right),\end{aligned} \tag{11}$$

where $\langle\chi|\eta\rangle_\rho$ is the density-weighted conditional mean scalar dissipation of mixture fraction. For the IEM model in the statistically stationary state, the PDF equation is

$$\begin{aligned}0 &= -\frac{\tilde{p}(\eta)}{\tau_{\text{res}}} + \frac{1}{\tau_{\text{res}}}\big[P\delta(\eta) + (1-P)\delta(1-\eta)\big] \\ &\quad - \frac{\partial}{\partial \eta}\left[\frac{1}{2\tau_{\text{mix}}}(\eta - \tilde{\xi})\tilde{p}(\eta)\right].\end{aligned} \tag{12}$$

By multiplying both sides of Eq. (12) by η and integrating from $-\infty$ to ∞, we obtain the formula for $\tilde{\xi}$ in the statistically stationary state:

$$\tilde{\xi} = 1 - P. \tag{13}$$

By multiplying both sides of Eq. (12) by $(\eta - \tilde{\xi})^2$ and integrating from $-\infty$ to ∞, we obtain the formula for $\widetilde{\xi''^2}$ in the statistically stationary state:

$$\widetilde{\xi''^2} = P(1-P)/(1 + \tau_{\text{res}}/\tau_{\text{mix}}). \tag{14}$$

In the PaSR, given the same values of P and $\tau_{\text{mix}}/\tau_{\text{res}}$, the Favre mean and variance (or the rms, ξ') of mixture fraction are the same for the IEM and MC models because they both conserve the mean of each component of the composition and make the variance of each component of the composition decay at the proper rate. So Eqs. (13) and (14) also apply to the MC model. The EMST model also conserves the mean of each component of the composition and consequently Eq. (13) also applies to the EMST model. But in the EMST model, the variance of each composition can decay at a different rate, while the amount of mixing performed is controlled so that the sum of the composition variances decays at the rate prescribed by τ_{mix}. Consequently, the decay of variance of mixture fraction for the EMST model is different from that in the IEM and MC models, but the difference is generally small. To a good approximation, we can also apply Eq. (14) to the EMST model.

Appendix B. Derivation of analytical solutions for the IEM model

In this section, for the IEM model when statistically stationary in the PaSR, we derive analytical expressions for the PDF of mixture fraction $\tilde{p}(\eta)$ and for the implied conditional mean scalar dissipation $\langle\chi|\eta\rangle_\rho$. The way to derive the expression for $\langle\chi|\eta\rangle_\rho$ is similar to the approach developed by Janicka and Peters [16].

For the IEM model, the evolution of mixture fraction for the ith particle is

$$\frac{d\xi^{(i)}}{dt} = -\frac{1}{2\tau_{\text{mix}}}\big(\xi^{(i)} - \tilde{\xi}\big), \tag{15}$$

where $\tilde{\xi} = 1 - P$. So the mixture fraction of each particle is a unique function of its age s:

$$\begin{aligned}\xi(s) &= (1-P)\left[1 - \exp\left(-\frac{s}{2\tau_{\text{mix}}}\right)\right] \quad \text{for } \xi(0) = 0, \\ &= 1 - P + P\exp\left(-\frac{s}{2\tau_{\text{mix}}}\right) \quad \text{for } \xi(0) = 1.\end{aligned} \tag{16}$$

And the age distribution is given by $f_{\text{age}}(s) = \frac{1}{\tau_{\text{res}}}\exp(-s/\tau_{\text{res}})$. So $\tilde{p}(\eta)$ is

$$\begin{aligned}\tilde{p}(\eta) &= \int_0^\infty f_{\text{age}}(s)\big[P\delta\big(\eta - \xi(s)|_{\xi(0)=0}\big) \\ &\qquad + (1-P)\delta\big(\eta - \xi(s)|_{\xi(0)=1}\big)\big]\,ds \\ &= \int_0^\infty \frac{1}{\tau_{\text{res}}}\exp\left(-\frac{s}{\tau_{\text{res}}}\right)\big\{P\delta\big(\eta - \xi(s)|_{\xi(0)=0}\big) \\ &\qquad + (1-P)\delta\big(\eta - \xi(s)|_{\xi(0)=1}\big)\big\}\,ds\end{aligned}$$

$$
\begin{aligned}
&= \int_0^\infty \frac{1}{\tau_{\mathrm{res}}} \exp\left(-\frac{s}{\tau_{\mathrm{res}}}\right) \\
&\quad \times \left\{ P\delta\left(\eta - (1-P)\left[1 - \exp\left(-\frac{s}{2\tau_{\mathrm{mix}}}\right)\right]\right) \right. \\
&\quad + (1-P)\delta \\
&\quad \left. \times \left(\eta - \left[1 - P + P\exp\left(-\frac{s}{2\tau_{\mathrm{mix}}}\right)\right]\right)\right\} ds \\
&= \frac{\lambda P}{(1-P)^\lambda}(1-P-\eta)^{\lambda-1} \\
&\qquad \text{for } 0 \leqslant \eta < 1-P, \\
&= \frac{\lambda(1-P)}{P^\lambda}\big[\eta - (1-P)\big]^{\lambda-1} \\
&\qquad \text{for } 1-P < \eta \leqslant 1, \qquad (17)
\end{aligned}
$$

where $\lambda = 2\tau_{\mathrm{mix}}/\tau_{\mathrm{res}}$. Note that $\eta = 1-P$ is a singular point. It is caused by the fact that in the IEM model it takes a particle an infinite time to reach the mean mixture fraction.

In the PaSR, when statistically stationary, from Eq. (11), we have

$$
\begin{aligned}
&\frac{\partial^2}{\partial\eta^2}\big(\tilde{p}(\eta)\langle\chi|\eta\rangle_\rho\big) \\
&\quad = \frac{2}{\tau_{\mathrm{res}}}\big[-\tilde{p}(\eta) + P\delta(\eta) + (1-P)\delta(1-\eta)\big]. \qquad (18)
\end{aligned}
$$

Integrating Eq. (18) from $-\infty$ to η, we obtain

$$
\begin{aligned}
\frac{\partial}{\partial\eta}\big(\tilde{p}(\eta)\langle\chi|\eta\rangle_\rho\big) &= \frac{2}{\tau_{\mathrm{res}}}\big[-F(\eta) + PH(\eta) \\
&\quad + (1-P)H(\eta-1)\big], \qquad (19)
\end{aligned}
$$

where $F(\eta)$ is the density-weighted cumulative distribution function of mixture fraction and $H(\eta)$ is the Heaviside function.

Integrating Eq. (19) from $-\infty$ to η ($0 \leqslant \eta \leqslant 1$), we obtain

$$
\langle\chi|\eta\rangle_\rho = \frac{2}{\tau_{\mathrm{res}}\tilde{p}(\eta)}\left(-\int_0^\eta F(\eta')\,d\eta' + P\eta\right). \qquad (20)
$$

This equation is used to determine $\langle\chi|\eta\rangle_\rho$ from the numerical calculation of $\tilde{p}(\eta)$ for the MC and EMST mixing models. For the IEM model, from Eq. (17), we obtain

$$
\begin{aligned}
F(\eta) &= P - \frac{P}{(1-P)^\lambda}(1-P-\eta)^\lambda \\
&\qquad \text{for } 0 \leqslant \eta < 1-P, \\
&= P + \frac{1-P}{P^\lambda}\big(\eta - (1-P)\big)^\lambda \\
&\qquad \text{for } 1-P < \eta \leqslant 1. \qquad (21)
\end{aligned}
$$

Substituting Eqs. (17) and (21) into Eq. (20), we obtain the expression for $\langle\chi|\eta\rangle_\rho$,

$$
\begin{aligned}
\langle\chi|\eta\rangle_\rho &= \frac{2[(1-P)^{\lambda+1} - (1-P-\eta)^{\lambda+1}]}{\tau_{\mathrm{res}}\lambda(\lambda+1)(1-P-\eta)^{\lambda-1}} \\
&\qquad \text{for } 0 \leqslant \eta < 1-P, \\
&= \frac{2[P^{\lambda+1} - (\eta-(1-P))^{\lambda+1}]}{\tau_{\mathrm{res}}\lambda(\lambda+1)(\eta-(1-P))^{\lambda-1}} \\
&\qquad \text{for } 1-P < \eta \leqslant 1, \qquad (22)
\end{aligned}
$$

where $\lambda = 2\tau_{\mathrm{mix}}/\tau_{\mathrm{res}}$. Note that $\eta = 1-P$ is also a singular point.

References

[1] R.S. Barlow, J.H. Frank, Proc. Combust. Inst. 27 (1998) 1087–1095.
[2] Q. Tang, J. Xu, S.B. Pope, Proc. Combust. Inst. 28 (2000) 133–139.
[3] J. Xu, S.B. Pope, Combust. Flame 123 (2000) 281–307.
[4] R.P. Lindstedt, S.A. Louloudi, E.M. Vaos, Proc. Combust. Inst. 28 (2000) 149–156.
[5] J. Villermaux, J.C. Devillon, in: Proc. 2nd Int. Symp. on Chemical Reaction Engineering, Elsevier, New York, 1972.
[6] C. Dopazo, E.E. O'Brien, Acta Astronaut. 1 (1974) 1239–1266.
[7] J. Janicka, W. Kolbe, W. Kollman, J. Nonequilib. Thermodyn. 4 (1977) 47–66.
[8] S. Subramaniam, S.B. Pope, Combust. Flame 115 (1998) 487–514.
[9] J.Y. Chen, Combust. Sci. Technol. 122 (1997) 63–94.
[10] S.M. Correa, Combust. Flame 93 (1993) 41–60.
[11] Z. Ren, S. Subramaniam, S.B. Pope, http://mae.cornell.edu/~laniu/emst.
[12] U. Maas, J. Warnatz, Proc. Combust. Inst. 22 (1988) 1695–1704.
[13] S.B. Pope, Combust. Theory Modell. 1 (1997) 41–63.
[14] A.Y. Klimenko, R.W. Bilger, Prog. Energy Combust. Sci. 25 (1999) 595–687.
[15] N. Peters, Turbulent Combustion, in: Cambridge Monographs on Mechanics, Cambridge Univ. Press, Cambridge, UK, 2000.
[16] J. Janicka, N. Peters, Proc. Combust. Inst. 19 (1982) 367–374.